**[The sediment green-blue color ratio as a proxy for biogenic silica productivity along the Chilean Margin.]**

[Chen Li[1,2*], Vincent J. Clementi[1*], Samantha C. Bova[1,3], Yair Rosenthal[1,4], Laurel B. Childress[5], James D. Wright[4], Zhimin Jian[2], and Expedition 379T Scientists†]

[[1]Department of Marine and Coastal Sciences, Rutgers University, New Brunswick, New Jersey, USA

[2]State Key Laboratory of Marine Geology, Tongji University, Shanghai, China

[3]Present address: Department of Geological Sciences, San Diego State University, San Diego, California, USA

[4]Department of Earth and Planetary Sciences, Rutgers University, New Brunswick, New Jersey, USA

[5]International Ocean Discovery Program, Texas A&M University, College Station, Texas, USA

†A list of authors and affiliations appears at the end of the paper]

## Contents of this file

Text S1 to S2
Figures S1 to S3
Tables S1 to S4

## Additional Supporting Information (Files uploaded separately)

Captions for data set S1 to S2 (upload as separate files)

## Introduction

Cores J1002 and J1007 were recovered from the Chilean Margin during the JR100 cruise (D/V JOIDES Resolution Expedition 379T) in 2019. All the experiments conducted in this study were performed at Department of Marine and Coastal Sciences, Rutgers University. This supporting information includes detailed description of biogenic silica measurement, data processing procedure and control points for J1002 and J1007 age models.

### Text S1.
### Biogenic Silica Measurement

In general, sediment samples were prepared with typical wet-alkaline digestion including "mineral correction" steps modified after Conley et al. (2001). Afterward, dissolved silica was measured by the molybdate blue spectrophotometric method using a modified procedure adapted from Mortlock et al. (1989).

A total of 22 and 41 samples were analyzed for J1002 and J1007, respectively. An addition of three J1001, six J1005 and four J1008 samples were measured. About 250 mg of freeze-dried sediments were homogenized using a mortar and pastel and placed in acid-cleaned 50 mL centrifuge tubes. Sediments were digested using 40 mL of 1 mol/L $Na_2CO_3$ solution in an 80 °C water bath. The tubes were shaken very quickly every 20 minutes for complete digestion. After 3 hours of digestion, the tubes were dipped in cool water for 5 minutes to stop the chemical reaction and then centrifuged for 2 minutes at 4200 rpm. Subsamples of 1 mL were taken from the upper solvent. Tubes were returned to the 80 °C water bath after vortex and sonication (1 minute). The subsampling procedure was repeated at the 4 and 5 h our marks of digestion time.

The molybdate reagent and the reducing reagent were prepared before the molybdate blue measurement. About 4.0 g of ammonium paramolybdate and 12 mL of concentrated HCl were dissolved in DI water, with a total volume of 500 mL. This solvent was further diluted with DI water (2:5/v:v) to the make molybdate reagent (pH ~ 1.2). The reducing reagent was a mixture of metol-sulfite solution (6 g of anhydrous sodium sulfite and 10 g of metol in 500 mL DI water), saturated oxalic acid solution, 50% sulphuric acid solution and DI water (5:3:3:4/v:v:v:v).

200 μL of the aforementioned subsample was pipetted into a 30 mL acid-cleaned plastic bottle containing 7 mL of molybdate reagent and mixed immediately. After 20 min, 3 mL of reducing reagent were added to the bottle and mixed rapidly. The bottles were capped and left to sit in the laminar flow hood for more than 12 hours for complete reduction.

Finally, the absorbance of the solution was measured in a 1-cm cell with an Algilent Cary 60 UV-Vis spectrophotometer peaked at 812 nm. Two operational blanks that went through digestion and molybdate blue procedures were analyzed for each batch.

**Text S2.**

**Data Processing and Evaluation**

The weight percentage of biogenic silica was calculated as:

SiOpal% = 112.4*F*(As-Ao)/M

where F is the slope resulted from standard calibration (F=2.763194); As and Ao refers to the absorbance of each subsample and operational blank, respectively; M stands for the weight of each sample in mg.

Percent biogenic opal was calculated as:

opal% = 2.4* SiOpal%

The "mineral correction" procedures were introduced to calibrate the contribution of mineral silicates. This continuous measurement requires a level of sophistication because subsampling is time sensitive and may result in possible mineral reprecipitation. During an ideal digestion, diatoms were quickly dissolved within 2 hours, while mineral silicates were slowly digested throughout the whole experiment.

A linear regression ($r^2$>0.6) was made for each sample based on the measured opal% of three subsamples versus digestion time, and the extrapolation to the intercept was taken as the corrected opal% for each sample (DeMaster, 1981). Corrected opal% show remarkable correlation ($r^2$=0.98) with 3-hour measured opal% for five Expedition 379T sites along the Chilean Margin (representing both open ocean and slope settings) (Figure S1, Table S1). It can be inferred that the contribution of mineral silicates is consistent for all samples under our digestion settings. Thus, the final opal% could be calculated as 3-hour measured opal% minus 0.3. A total of 14 duplicates was measured for the wet-alkaline digestion, yielding a standard error of 0.35%.

Prominent low values of magnetic susceptibility were found in certain intervals of J1002 and J1007. These intervals were thought to be affected by possible reworking or dissolution. Eight samples from J1007 and one sample from J1002 at these intervals were thought to have underestimated opal contents (Table S2).
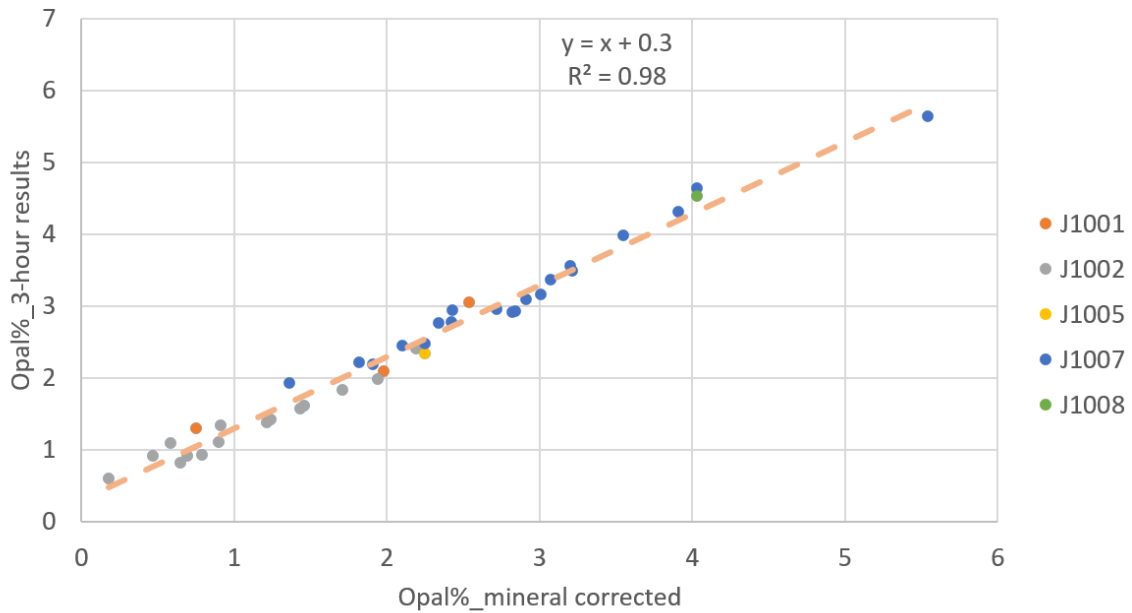
**Figure S1.** Mineral corrected opal% show remarkable correlation ($r^2$=0.98) with 3-hour measured opal% at five sites along the Chilean Margin.
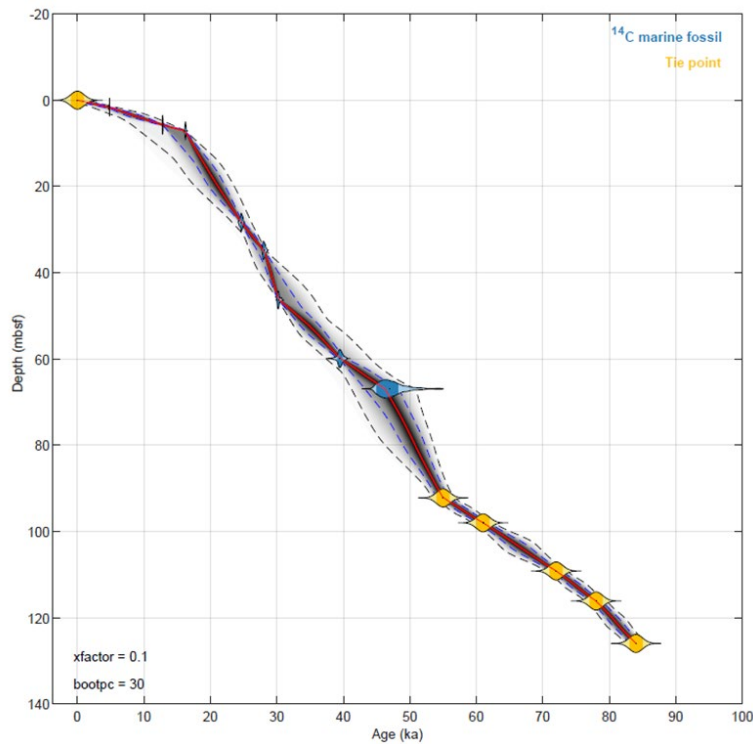


**Figure S2.** Depth-age relationship of Site J1002 from Undatable program (Lougheed et al., 2019). Yellow marks show the tie points of visual correlation between J1002 benthic *Uvigerina* spp. $\delta^{18}$O and LR04 benthic stack (Lisiecki and Raymo, 2005). Blue marks are the $^{14}$C ages derived from planktonic foraminifera (*Globigerina bulloides*).
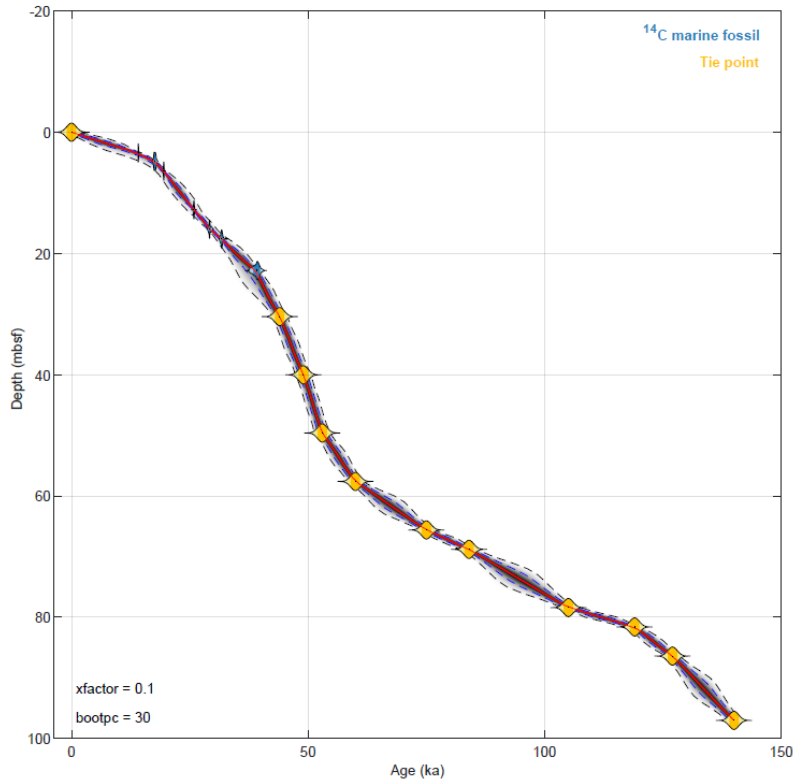
**Figure S3.** Depth-age relationship of Site J1007 from Undatable program (Lougheed et al., 2019). Yellow marks show the tie points of visual correlation between J1007 benthic *Uvigerina* spp. δ<sup>18</sup>O and LR04 benthic stack (Lisiecki and Raymo, 2005). Blue marks are the <sup>14</sup>C ages derived from planktonic foraminifera (*Globigerina bulloides*).

**Table S1.** Mineral corrected opal% vs 3-hour measured opal%.

| SITE | mineral corrected opal% | opal%_3-hour results |
|---|---|---|
| J1001 | 0.75 | 1.3 |
| J1001 | 1.98 | 2.1 |
| J1001 | 2.54 | 3.05 |
| J1002 | 0.18 | 0.6 |
| J1002 | 0.47 | 0.92 |
| J1002 | 0.58 | 1.09 |
| J1002 | 0.65 | 0.82 |
| J1002 | 0.69 | 0.91 |
| J1002 | 0.79 | 0.93 |
| J1002 | 0.9 | 1.11 |
| J1002 | 0.91 | 1.34 |
| J1002 | 1.21 | 1.38 |
| J1002 | 1.24 | 1.42 |
| J1002 | 1.43 | 1.57 |
| J1002 | 1.46 | 1.62 |

| | | |
|---|---|---|
| J1002 | 1.71 | 1.83 |
| J1002 | 1.94 | 1.99 |
| J1002 | 2.19 | 2.41 |
| J1005 | 2.25 | 2.34 |
| J1007 | 1.36 | 1.93 |
| J1007 | 1.82 | 2.22 |
| J1007 | 1.91 | 2.19 |
| J1007 | 2.1 | 2.45 |
| J1007 | 2.25 | 2.48 |
| J1007 | 2.34 | 2.76 |
| J1007 | 2.42 | 2.78 |
| J1007 | 2.43 | 2.94 |
| J1007 | 2.72 | 2.96 |
| J1007 | 2.82 | 2.92 |
| J1007 | 2.84 | 2.93 |
| J1007 | 2.91 | 3.1 |
| J1007 | 3.01 | 3.17 |
| J1007 | 3.07 | 3.37 |
| J1007 | 3.2 | 3.56 |
| J1007 | 3.21 | 3.49 |
| J1007 | 3.55 | 3.98 |
| J1007 | 3.91 | 4.32 |
| J1007 | 4.03 | 4.64 |
| J1007 | 5.54 | 5.64 |
| J1008 | 4.03 | 4.54 |

**Table S2.** Measured opal% for Site J1002 and J007.

| Site | Depth | Age | GB | OPAL | notes |
|---|---|---|---|---|---|
| J1002 | 0.105 | 0.30 | 1.232 | 4.36 | |
| J1002 | 1.605 | 4.48 | 1.262 | 2.11 | |
| J1002 | 2.905 | 7.24 | 1.224 | 2.87 | |
| J1002 | 4.305 | 9.98 | 1.207 | 2.61 | |
| J1002 | 5.705 | 12.84 | 1.139 | 1.69 | |
| J1002 | 7.105 | 15.98 | 1.123 | 1.07 | |
| J1002 | 36.192 | 28.35 | 1.018 | 0.63 | |
| J1002 | 43.194 | 29.69 | 1.003 | 0.36 | |
| J1002 | 59.883 | 39.60 | 1.114 | 0.91 | |
| J1002 | 61.303 | 40.92 | 1.05 | 0.7 | |
| J1002 | 64.113 | 43.55 | 1.088 | 0.81 | |
| J1002 | 92.216 | 55.12 | 1.199 | 1.45 | |
| J1002 | 121.762 | 81.39 | 1.039 | 1.53 | |

| | | | | | |
|---|---|---|---|---|---|
| J1002 | 124.482 | 83.04 | 1.12 | 1.04 | |
| J1007 | 0.11 | 0.44 | 1.185 | 3.54 | |
| J1007 | 6.409 | 19.37 | 1.169 | 2.8 | |
| J1007 | 9.609 | 22.64 | 1.116 | 1.92 | |
| J1007 | 11.209 | 24.25 | 1.108 | 1.89 | |
| J1007 | 12.803 | 25.89 | 1.079 | 2.63 | |
| J1007 | 14.393 | 27.61 | 1.126 | 4.34 | |
| J1007 | 22.375 | 38.11 | 1.187 | 3.8 | |
| J1007 | 25.606 | 40.64 | 1.162 | 3.81 | |
| J1007 | 27.236 | 41.65 | 1.183 | 3.91 | |
| J1007 | 33.599 | 45.72 | 1.189 | 4.9 | |
| J1007 | 41.606 | 49.70 | 1.137 | 3.41 | |
| J1007 | 43.206 | 50.38 | 1.186 | 4.34 | |
| J1007 | 48.001 | 52.29 | 1.238 | 5.34 | |
| J1007 | 49.605 | 53.11 | 1.177 | 5.35 | |
| J1007 | 60.801 | 66.01 | 1.098 | 2.4 | |
| J1007 | 67.197 | 79.48 | 1.121 | 2.87 | |
| J1007 | 70.298 | 87.32 | 1.185 | 2.83 | |
| J1007 | 72.003 | 91.02 | 1.129 | 2.77 | |
| J1007 | 75.203 | 97.94 | 1.135 | 3.53 | |
| J1007 | 81.596 | 118.31 | 1.186 | 3.65 | |
| J1007 | 89.602 | 130.97 | 1.146 | 2.85 | |
| J1007 | 99.979 | 143.95 | 1.224 | 3.74 | |
| J1002 | 104.965 | 67.80 | 1.04 | 0.62 | Data points with underestimated opal contents. |
| J1007 | 1.605 | 6.44 | 1.208 | 2.2 | Data points with underestimated opal contents. |
| J1007 | 1.615 | 6.48 | 1.22 | 2.55 | Data points with underestimated opal contents. |
| J1007 | 3.205 | 12.87 | 1.187 | 1.99 | Data points with underestimated opal contents. |
| J1007 | 52.005 | 55.16 | 1.243 | 3.03 | Data points with underestimated opal contents. |
| J1007 | 52.805 | 55.84 | 1.25 | 3.97 | Data points with underestimated opal contents. |
| J1007 | 53.605 | 56.49 | 1.253 | 2.53 | Data points with underestimated opal contents. |
| J1007 | 54.405 | 57.15 | 1.215 | 1.98 | Data points with underestimated opal contents. |
| J1007 | 93.838 | 136.04 | 1.207 | 2.74 | Data points with underestimated opal contents. |

**Table S3.** Age control points for J1002 and J1007.

| Site | Depth (mbsf) | Uncrorrected Age (yr) | Age error (yr) | Date type | Calibration |
|------|------|------|------|------|------|
| J1002 | 0 | 0 | | core-top | None |
| J1002 | 1.605 | 4245 | 25 | 14C_age | IntCal20 |
| J1002 | 5.705 | 10925 | 40 | 14C_age | IntCal20 |
| J1002 | 7.105 | 13475 | 45 | 14C_age | IntCal20 |
| J1002 | 28.305 | 20490 | 90 | 14C_age | IntCal20 |
| J1002 | 34.792 | 23950 | 110 | 14C_age | IntCal20 |
| J1002 | 46.284 | 26000 | 160 | 14C_age | IntCal20 |
| J1002 | 59.883 | 34310 | 370 | 14C_age | IntCal20 |
| J1002 | 66.918 | 44000 | 1600 | 14C_age | IntCal20 |
| J1002 | 92.22 | 55000 | | tie point | None |
| J1002 | 97.99 | 61000 | | tie point | None |
| J1002 | 109.16 | 72000 | | tie point | None |
| J1002 | 116.12 | 78000 | | tie point | None |
| J1002 | 125.96 | 84000 | | tie point | None |
| J1007 | 0 | 0 | | core-top | None |
| J1007 | 3.41 | 12230 | 35 | 14C_age | IntCal20 |
| J1007 | 4.797 | 14430 | 140 | 14C_age | IntCal20 |
| J1007 | 6.409 | 16150 | 70 | 14C_age | IntCal20 |
| J1007 | 12.79 | 21570 | 130 | 14C_age | IntCal20 |
| J1007 | 15.99 | 24970 | 170 | 14C_age | IntCal20 |
| J1007 | 17.583 | 27820 | 190 | 14C_age | IntCal20 |
| J1007 | 22.765 | 34080 | 480 | 14C_age | IntCal20 |
| J1007 | 30.408 | 44000 | | tie point | None |
| J1007 | 40.006 | 49000 | | tie point | None |
| J1007 | 49.605 | 53000 | | tie point | None |
| J1007 | 57.601 | 60000 | | tie point | None |
| J1007 | 65.602 | 75000 | | tie point | None |
| J1007 | 68.797 | 84000 | | tie point | None |
| J1007 | 78.399 | 105000 | | tie point | None |
| J1007 | 81.596 | 119000 | | tie point | None |
| J1007 | 86.4 | 127000 | | tie point | None |
| J1007 | 97.008 | 140000 | | tie point | None |

**Table S4.** Measured $C_{org}$% for J1007.

| Depth_CCSF_m | G/B | Corg% | |
|------|------|------|------|
| 0.1 | 1.182 | 2.38 | |
| 0.11 | 1.185 | 2.02 | |
| 4.797 | 1.141 | 0.67 | |

| | | | |
|---|---|---|---|
| 6.409 | 1.169 | 0.76 | |
| 8.009 | 1.088 | 0.75 | |
| 9.609 | 1.116 | 0.8 | |
| 11.209 | 1.108 | 0.87 | |
| 12.803 | 1.079 | 0.74 | |
| 14.393 | 1.126 | 0.92 | |
| 16.003 | 1.133 | 1.11 | |
| 17.61 | 1.17 | 1.08 | |
| 19.21 | 1.163 | 1.06 | |
| 20.83 | 1.187 | 0.92 | |
| 22.375 | 1.187 | 0.99 | |
| 24.006 | 1.171 | 0.97 | |
| 25.606 | 1.162 | 1.19 | |
| 27.236 | 1.183 | 1.03 | |
| 28.808 | 1.161 | 0.9 | |
| 30.408 | 1.179 | 1 | |
| 32.008 | 1.192 | 1.09 | |
| 33.599 | 1.189 | 1.13 | |
| 35.199 | 1.166 | 0.71 | |
| 36.799 | 1.172 | 0.73 | |
| 38.399 | 1.141 | 0.76 | |
| 40.006 | 1.128 | 0.82 | |
| 41.606 | 1.137 | 0.92 | |
| 44.801 | 1.178 | 1 | |
| 46.401 | 1.165 | 1.24 | |
| 48.001 | 1.238 | 1.92 | |
| 49.605 | 1.177 | 1.63 | |
| 50.405 | 1.196 | 1.3 | |
| 51.205 | 1.216 | 2.19 | |
| 55.205 | 1.203 | 0.81 | |
| 56.001 | 1.236 | 0.75 | |
| 56.806 | 1.168 | 0.64 | |
| 57.601 | 1.172 | 0.73 | |
| 59.201 | 1.126 | 0.6 | |
| 60.801 | 1.098 | 0.64 | |
| 62.402 | 1.162 | 0.81 | |
| 64.002 | 1.187 | 0.73 | |
| 64.802 | 1.169 | 0.73 | |
| 65.602 | 1.151 | 0.67 | |
| 67.197 | 1.121 | 0.71 | |
| 68.797 | 1.093 | 0.6 | |
| 70.298 | 1.185 | 0.66 | |

| | | | |
|---|---|---|---|
| 72.003 | 1.129 | 0.69 | |
| 73.603 | 1.167 | 0.7 | |
| 74.303 | 1.168 | 0.66 | |
| 74.803 | 1.116 | 0.66 | |
| 75.203 | 1.135 | 0.7 | |
| 75.703 | 1.152 | 0.68 | |
| 76.204 | 1.172 | 0.68 | |
| 76.799 | 1.18 | 0.71 | |
| 78.399 | 1.147 | 0.71 | |
| 79.996 | 1.188 | 0.84 | |
| 80.501 | 1.265 | 0.94 | |
| 81.001 | 1.238 | 0.93 | |
| 81.596 | 1.186 | 0.8 | |
| 83.2 | 1.189 | 0.8 | |
| 84.8 | 1.186 | 0.7 | |
| 86.4 | 1.126 | 0.58 | |
| 87.86 | 1.171 | 0.68 | |
| 89.602 | 1.146 | 0.73 | |
| 92.202 | 1.178 | 0.97 | |
| 95.408 | 1.287 | 1.49 | |
| 97.008 | 1.214 | 0.64 | |
| 98.609 | 1.201 | 0.67 | |
| 99.979 | 1.224 | 0.93 | |
| 102.419 | 1.111 | 0.78 | |
| 103.413 | 1.136 | 0.6 | |
| 105.013 | 1.157 | 0.59 | |
| 106.613 | 1.124 | 0.53 | |
| 108.213 | 1.118 | 0.58 | |
| 111.454 | 1.084 | 0.61 | |
| 113.019 | 1.128 | 0.59 | |
| 114.615 | 1.217 | 1.15 | |
| 116.215 | 1.194 | 0.83 | |
| 117.815 | 1.234 | 0.9 | |
| 119.005 | 1.181 | 0.74 | |
| 1.605 | 1.208 | 1.72 | Data points with underestimated opal contents. |
| 1.615 | 1.22 | 1.86 | Data points with underestimated opal contents. |
| 3.205 | 1.187 | 1.16 | Data points with underestimated opal contents. |
| 52.005 | 1.243 | 1.27 | Data points with underestimated opal contents. |

| | | | |
|---|---|---|---|
| 52.805 | 1.25 | 1.43 | Data points with underestimated opal contents. |
| 53.605 | 1.253 | 1.25 | Data points with underestimated opal contents. |
| 54.405 | 1.215 | 0.9 | Data points with underestimated opal contents. |
| 93.838 | 1.207 | 0.89 | Data points with underestimated opal contents. |

**Data Set S1.** Site J1007 G/B, reconstructed opal%, linear sedimentation rate and opal mass accumulation rate data.

**Data Set S2.** Site J1002 G/B, reconstructed opal% data.

**References**
Conley, D. J., & Schelske, C. L. (2001). Biogenic Silica. In J. P. Smol, H. J. B. Birks, W. M. Last, R. S. Bradley, & K. Alverson (Eds.), Tracking Environmental Change Using Lake Sediments: Terrestrial, Algal, and Siliceous Indicators (pp. 281-293). Dordrecht: Springer Netherlands.
DeMaster, D. J., 1979. The marine budgets of silica and Ph.D. Dissertation, Yale University, 308 pp.
Lisiecki, L. E., & Raymo, M. E. (2005). A Pliocene-Pleistocene stack of 57 globally distributed benthic δ18O records. Paleoceanography, 20(1), n/a-n/a. doi:10.1029/2004pa001071
Lougheed, B. C., & Obrochta, S. P. (2019). A Rapid, Deterministic Age-Depth Modeling Routine for Geological Sequences With Inherent Depth Uncertainty. Paleoceanography and Paleoclimatology, 34(1), 122-133. doi:10.1029/2018pa003457
Mortlock, R. A., & Froelich, P. N. (1989). A simple method for the rapid determination of biogenic opal in pelagic marine sediments. Deep Sea Research Part A. Oceanographic Research Papers, 36(9), 1415-1426. doi:https://doi.org/10.1016/0198-0149(89)90092-7